KSCE Journal of Civil Engineering (2022) 26(9):3764-3775
DOI 10.1007/s12205-022-1493-3

pISSN 1226-7988, eISSN 1976-3808
www.springer.com/12205

Geotechnical Engineering

Field Investigation and Dynamic Process Simulation: A Case Study of Rock Avalanche in Pusa Village, Nayong County, Guizhou Province, China

Zhong Fu Wang[a,b], Handong Liu[a], Riyun Li[a], Yunfeng Fang[c], and Dan Bi[d]

[a]*College of Geosciences and Engineering, North China University Resources and Electric Power,, Zhengzhou 450046, China*
[b]*Levee Safety and Disaster Prevention Engineering Research Center of Ministry of Water Resources, Zhengzhou 450099, China*
[c]*Zhejiang Huadong Construction Engineering Co., Ltd., Hangzhou 310014, China*
[d]*CNPC Liaohe Engineering Co., Ltd., Panjin 124010, China*

ARTICLE HISTORY

Received 19 August 2021
Revised 22 November 2021
Accepted 5 April 2022
Published Online 19 July 2022

KEYWORDS

Rock avalanche
Influence factor
Failure mechanism
Numerical simulation
Dynamic process

ABSTRACT

This paper geologically analyzed and numerically simulated the rock avalanche which happened in Pusa Village, Zhangjiawan Town, Nayong County, Guizhou Province, China on 28 August 2017, with approximately 5×10^5 m^3 of failure mass. The features, dynamic process and evolution mechanism of the Pusa avalanche, based on the detailed field geological survey, UAV photography and monitoring video, was analyzed in detail, and the numerical model was established to simulate the initiation-movement-accumulation process. The results show that the rock avalanche originated basically from the limestone and siltstone of Yelong Formation, Triassic which extend approximately horizontally and possess developed dissolution and subsidence. The joints within such strata have progressively evolved into fissure belt and subsidence belt resulting from long-term weathering, and the steep joints parallel to slope surface were developed due to the tectonic and unloading actions. The slope deformed and fractured because of long-term gravity and weathering actions, and meanwhile the rainstorm and mining activity accelerated the deformation of slope, which finally resulted in the overall instability of slope. The in-depth analysis to the generation and disaster-induced mechanism of Pusa avalanche is of great importance to the prevention of such accidents.

1. Introduction

Rock avalanches are geological phenomenon triggered by various factors such as rainstorm, earthquake and human activities, and extensively occur in mountainous or hilly regions. They not only play an important role in landform evolution but also generally results in heavy casualty and catastrophic damage to infrastructures and residential properties (Smith et al., 2005; Zhu et al., 2005; Zambrano, 2007; Bozzano et al., 2011; Dai et al., 2011; Wu et al., 2013; Cox et al., 2015; Haque et al., 2019). Since 2000, many rock avalanches have happened in southwestern China, such as 2000 Yigong landslide in Tibet (Huang, 2004), 2009 Wulong landslide in Chongqing (Yin, 2010; Li et al., 2020), 2017 Mao County high-speed long-runout landslide in Sichuan Province and 2017 Pusa landside in Zhangjiawan Town, Nayong County, Guizhou Province (He et al., 2017; Xu et al., 2017; Fan et al., 2019). Rock avalanches generally occur abruptly and rarely, with short duration, rapid disaster generation and catastrophic damage. Therefore, the dynamic process of rock avalanches is usually difficultly captured by video camera, and few witnesses can survive from such accidents. As a consequence, high-speed long-runout rock avalanches were generally analyzed based on the field investigation and historical data (Jibson et al., 2006; Hewitt, 2009; Pirulli, 2009; Socco et al., 2010).

A rock avalanche of collapse-landslide mode occurred at about 10:30 local time on August 28, 2017 in Pusa Village, Zhangjiawan Town, Nayong County, Guizhou Province, China (N26.63°, E105.45°). About 5×10^5 m^3 disintegrated rock detached from a mountain ridge, collided against the slope surface, and moved rapidly downward in the form of rock avalanche. The avalanche slid over the original loose debris, and finally stopped in Pusa Village due to the obstruction of rural houses, which resulted in 35 deaths and 8 injuries. The accumulation is about 810 m long, and around 380 m wide at the middle, with volume

CORRESPONDENCE Zhong Fu Wang xfjtwzf@163.com College of Geosciences and Engineering, North China University Resources and Electric Power, Zhengzhou 450046, China

of approximately $8 \times 10^5 m^3$ (Xiao et al., 2018; Chen et al., 2020).

In this study the failure mechanism and inducing factors of the above Pusa avalanche was analyzed to determine the scale, accumulation range and distribution characteristics according to data collection, field investigation, engineering geological mapping and UAV aerial photography. Combined with the precious video of Pusa avalanche, a numerical model for simulating the dynamic process of rock avalanche-debris flow is established by using the shallow water equations, and then the dynamic evolution law for disaster generation, avalanche movement and debris accumulation is studied.

2. Study Area

2.1 Physical Geography

The study area is located in Pusa Village, Zhangjiawan Town, Nayong County, Bijie City, Guizhou Province, China (N26° 38′ 21″, E105° 26′ 42″), approximately 6 km away from Zhangjiawan Town, around 31 km from Nayong County, and about 170 km from Guiyang, the capital of Guizhou Province.

The study area belongs to the humid and warm subtropical monsoon climate, with abundant rainfall, and has the average annual temperature of 11°C and average annual precipitation of 1,200 to 1,300 mm, with most rainfall in June and July. In 2017, the study area suffered from the rainfall of up to 161.6 mm in June, 228.7 mm in July, but only 44.3 mm in August. Statistical results indicate that there was no rainfall during the period of three days before avalanche.

2.2 Engineering Geology

2.2.1 Terrain and Landform

The study area is situated in the second terrace of Yunnan-Guizhou Plateau in the western Guizhou, and features low to middle mountainous landform of tectonic erosion and denudation. The mountains in the study area are generally high and steep, and basically extend southwestward, generally with high elevation in the southern part and low elevation in the northern part. The mountain ridge in the area consists basically of the Yelang Formation, lower Triassic, with the maximum elevation of 2,175 m at the slope top in the southwestern study area and minimum elevation of 1,875 m at the stream bottom near Pusa Village. The upper part of the slope in the study area is steep while the lower part is gentle, with slope angle of 10 – 25°, partially up to 55°, and the height difference of about 300 m. The slope foot features an about 1 km long gentle platform. The coal strata in the lower part belongs to the Longtan Formation, upper Permian, and the coal seam outcrop is generally flat, with elevation of 1,700 – 1,900 m, averagely about 1,850 m. Most coal stratum is covered

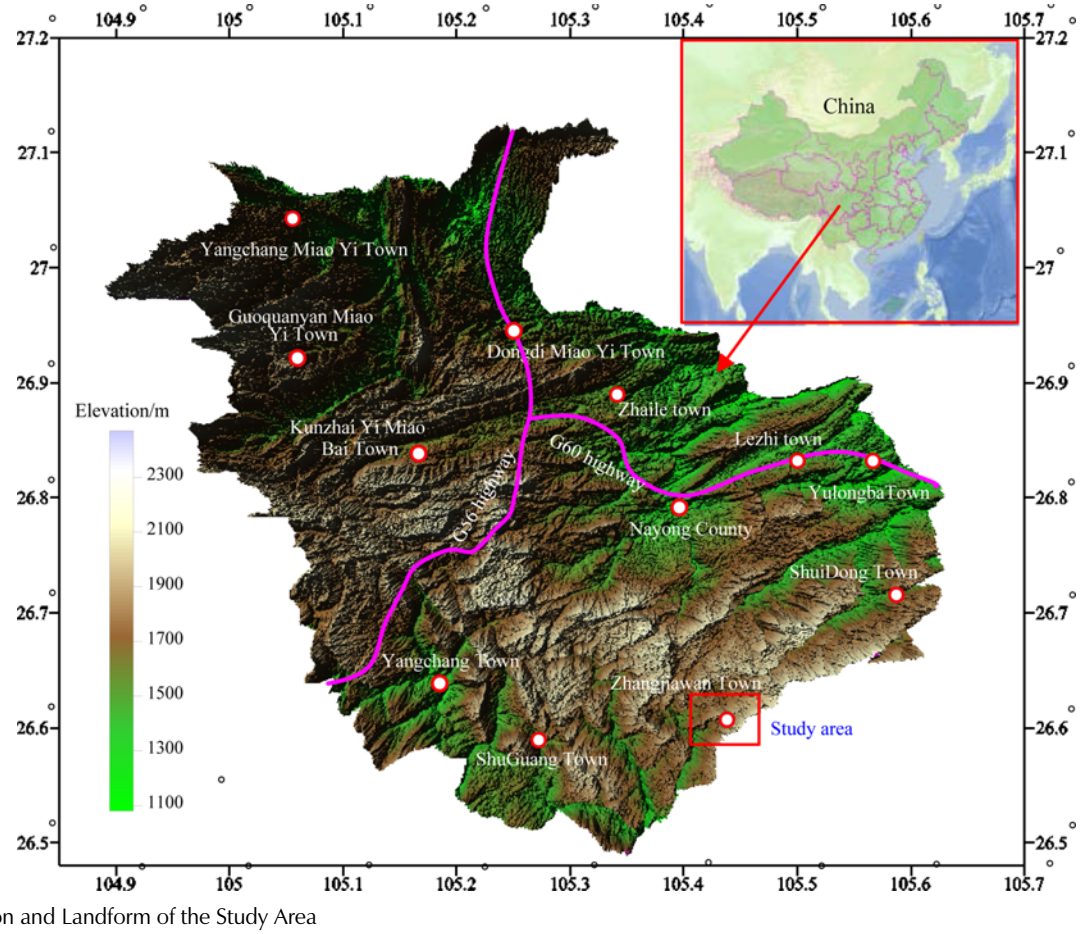

Fig. 1. Location and Landform of the Study Area

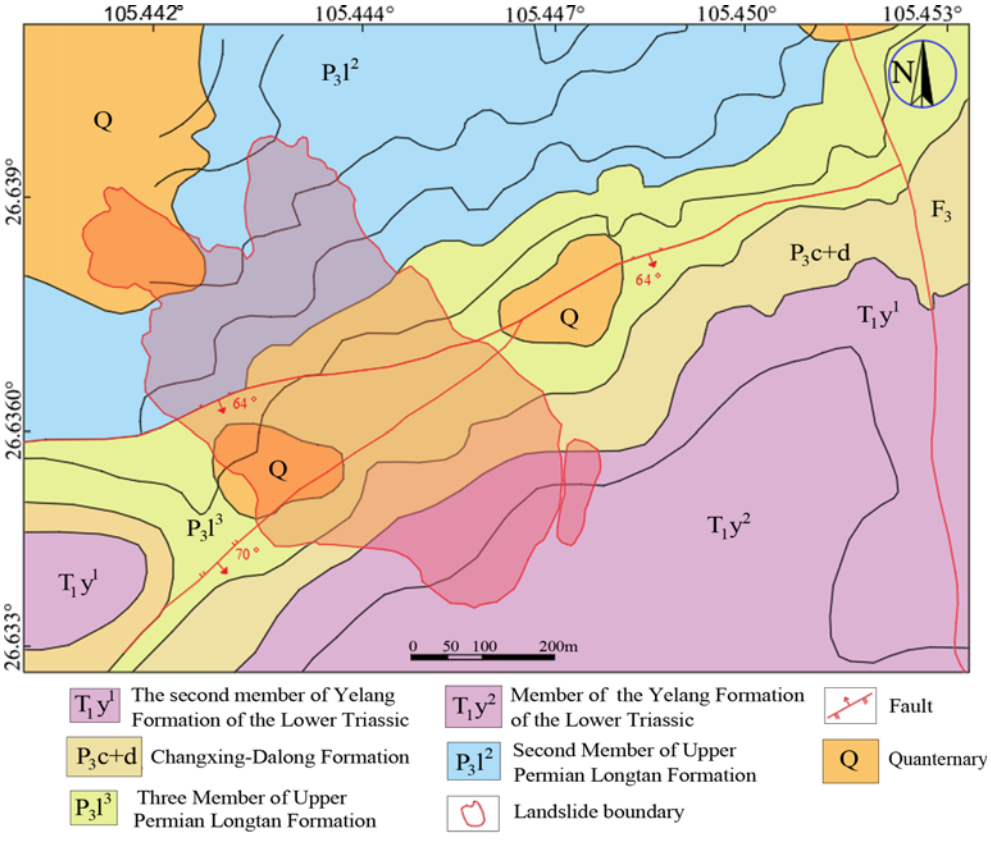

Fig. 2. Geological Map of the Study Area

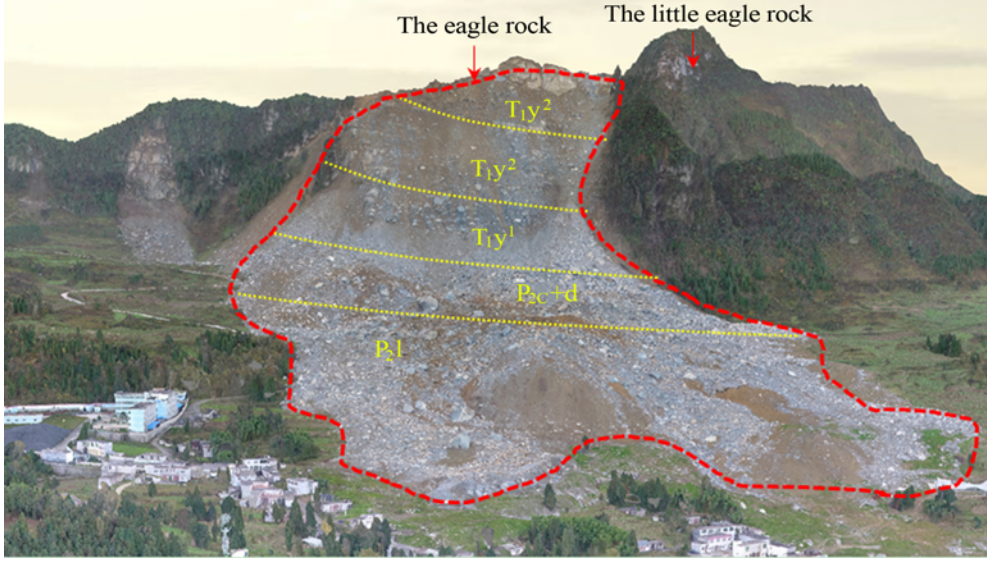

Fig. 3. Schematic Geological Condition of the Pusa Rock Avalanche

by the Quaternary layer which is commonly covered with farmland and residential houses.

2.2.2 Lithology

The outcrops consist of the Quaternary, Yelong Formation of lower Triassic, Changxin-Dalong Formation of Permian, and Longtan Formation of Permian, and the ground is generally covered by the Quaternary layer (Q). The upper part of Yelong Formation (T_1y) consists of cyan grey to grey brown, thin to moderately thick limestone, and the lower part grey siltstone. The Changxin-Dalong Formation (P_2c+d) consists of grey argillaceous limestone, and has conformable contact with Yelong Formation (T_1y). The Longtan Formation (P_3l) is paralic facies, and consists mainly of grey to dark grey argillaceous siltstone

with coal and thin layer of carbonaceous shale. Various coal-bearing outcrops can be found in the study area.

2.2.3 Geological Structure

The study area is located in the NW limb of a regional syncline, and belongs to monoclonal structure. The attitudes of coal seam are identical to those of strata, and the strata attitudes vary greatly due to the influence of fault structure, with dip direction of 138 – 187° and dip angle of 7 – 10°. There are three faults near the study area, namely, F1, F2 and F3. F1 is a normal fault, with NE strike, dip direction of 155 – 167° and dip angle of 63 – 70°, and its east end is in contact with F3. F2 is a reverse fault, with SE dip direction and dip angle of 70 – 75°. F3 is a normal fault, with NE dip direction and dip angle of 75 – 80°. F1 and F2 cross the avalanche accumulation region, and F3 is about 500 m east of the initial position of rock avalanche.

2.2.4 Hydrogeology

The T_1y limestone is soluble, but the P_2c+d and P_3l strata are not soluble. The sinkholes and collapses are developed in the limestone outcrop region, and the rainfall can rapidly recharge the groundwater through sinkholes and shafts. In the region without soluble outcrop, the rainfall recharges the groundwater by infiltration through rock fractures and voids. The upper part of avalanche source is soluble, while the lower part is not soluble. The rainfall infiltration through sinkholes and shafts is beneficial to the groundwater recharge.

3. Zonation and Dynamic Process

As a large-scale avalanche, the Pusa avalanche area can be divided into the source zone, scraping zone, and accumulation zone in terms of deformation. The previoused fractured rocks detached from the upper part, scraped the loose deposit in the middle part in the form of avalanche along 300 – 310° direction, and finally accumulated in the slope foot and platform in an irregular fan shape. The accumulation buried some village houses, and is horizontally about 800 – 820 m long, with thickness of

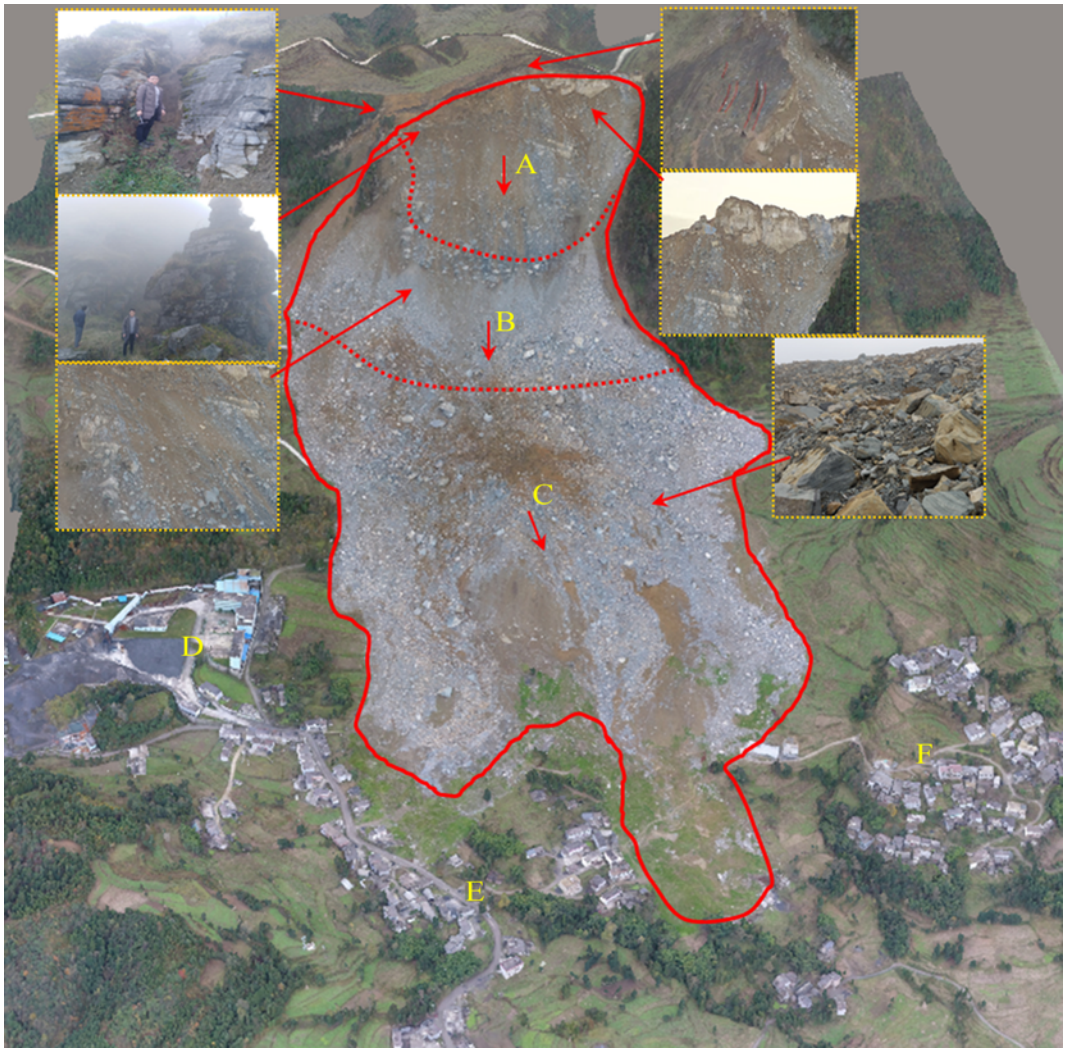

Fig. 4. Bird View of Pusa Avalanche (A. Source Zone; B. Scraping Zone; C. Accumulation Zone; D. Coal Mine; E. Residential Area; F. Residential Area)

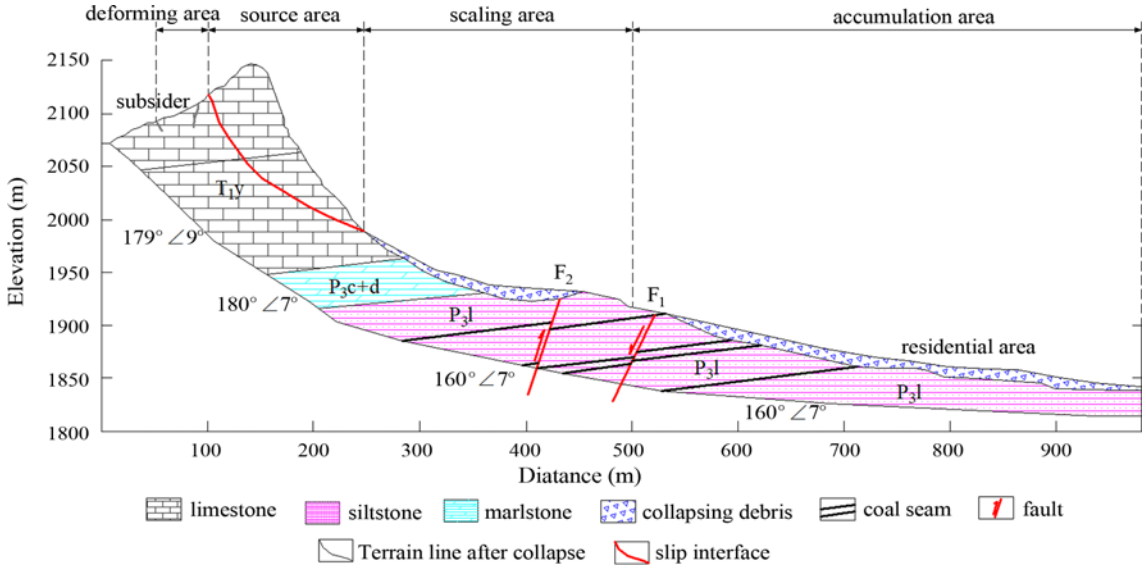

Fig. 5. Engineering Geological Profile of Pusa Rock Avalanche

averagely about 4 m. The avalanche volume originated from the source zone is about 49.1 × 10^4 m^3, the volume scraped from the scraped zone is around 2.1 × 10^4 m^3, and the volume scraped from the accumulation zone is approximately 31 × 10^4 m^3. Therefore, the Pusa avalanche totals about 82.4 × 10^4 m^3 in volume.

3.1 Source Zone

The source zone is located at the upper part of the mountain slope, with elevation of 1990 – 2147 m. The toe of slide surface is about 180 m wide, with elevation of around 2,040 m and height difference of about 100 m. Before the avalanche happened, the slope is up to 55 – 70°. The strike of slope is approximately N40°E, and the attitude of strata is N80°E-EW/SE ∠ 5° – 7°. The strata incline slightly inward, with marl-bearing limestone in the upper part and siltstone-bearing sandy mudstone in the lower part. The lower part of the source zone subsided, and the upper part failed gradually due to the gravity in the similar form of toppling immediately before the avalanche occurred. After the rock avalanche, almost vertical escarpment can be found in the tail and steep slope with approximately plain surface can be observed in the lower part.

3.2 Scraping Zone

The scraping zone is generally located in the elevation of 1,920 – 1,990 m, with slope angle of 10 – 25°. There is a platform in the middle, slightly higher than two sides which are connected to nearby depression terrain. The bottom elevation of this zone is about 1,937 m, and the height difference between the toe of slide surface and the slope toe is around 100 m. Thus, the avalanche had great potential energy due to the large volume and high position. The scraping of avalanche against the ground further caused the increase in the avalanche volume. After the detached rocks collided against the ground, the high-speed long-runout avalanche formed along the depression terrain at two sides.

3.3 Accumulation Zone

The accumulation zone is basically in the 1,920 – 1,842 m elevation, and was originally formed as a gentle platform, with depression terrain and ditches on the left, where is the residential community of Pusa Village. The accumulation zone is approximately 600 m long and 410 m wide, gentle in the front and relatively steep in the tail. The strong collision during movement further disintegrated the detached rocks, which broken the accumulation body. The accumulation consists mainly of mudstone and some limestone. The rocks on the accumulation surface are relatively large, about 50 – 150 cm long, and some huge rocks are up to 5 – 6 m.

3.4 Dynamic Process of Failure

Luckily, the Pusa avalanche was captured by means of precious video at the front view and side view, as shown in Fig. 6. It originated from the northern small-scale collapse, and then developed from the small-scale collapse in the top and bottom of source zone. During the collapse, the stresses in the slope adjusted continuously, and rocks increasingly detached from the northern slope. The slope surface became concave, which may result from the increasing width of northern tension cracks. As a consequence, the southern slope began to deform, the rock mass in the bottom of source zone was pressed into broken belt as the boundary of source zone. The large-scale avalanche occurred in the form of general instability along the broken belt due to gravity.

The avalanche strongly collided against the earlier deposit due to the steep terrain. Although the rock disintegration and collision consumed some potential energy, the avalanche continued to move downward after collision at high speed because of the large volume and about 200 m height of avalanche, finally resulting in a catastrophe of 35 deaths and 8 injuries.

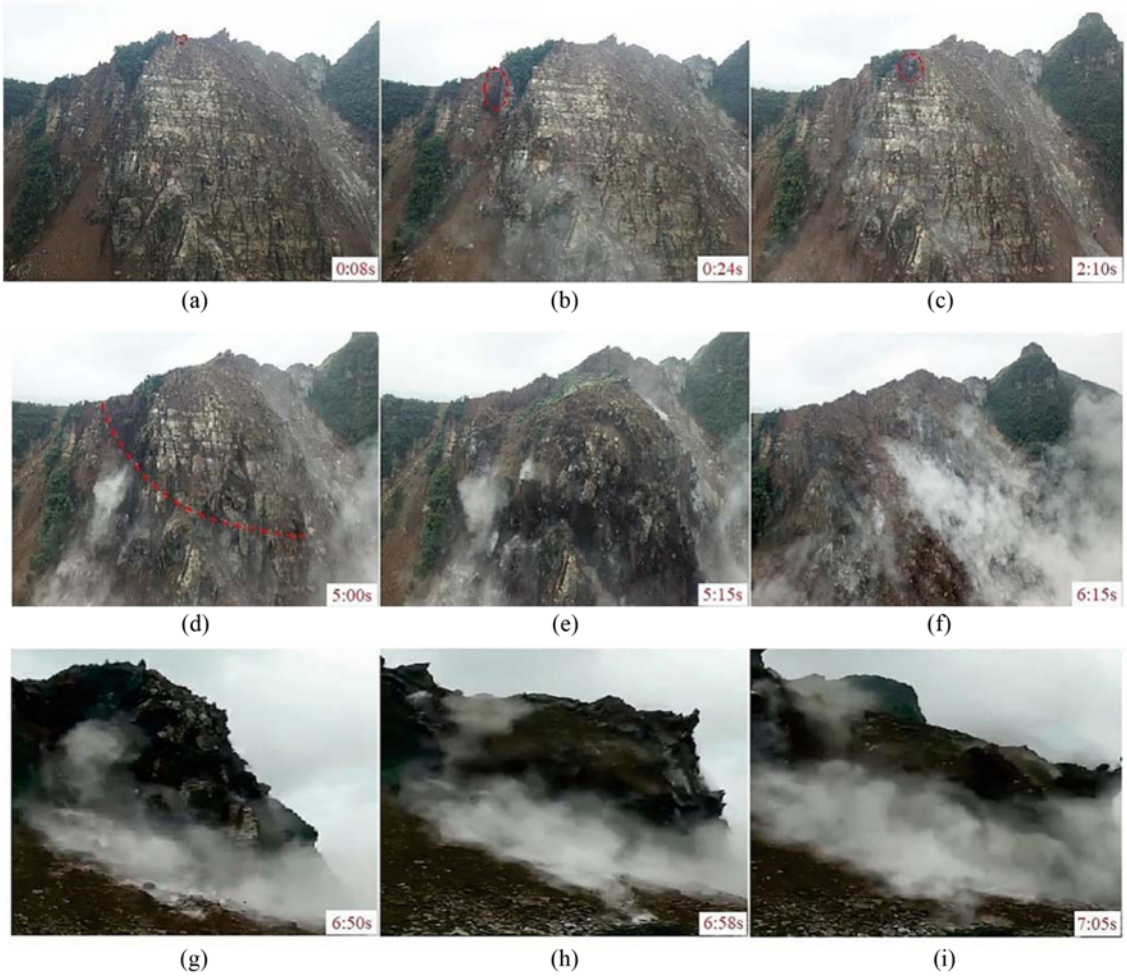

Fig. 6. The Failure of Rock Avalanche at Different Times: (a) 0:08s, (b) 0:24s, (c) 2:10s, (d) 5:00s, (e) 5:15s, (f) 6:15s, (g) 6:50s, (h) 6:58s, (i) 7:05s

4. Formation Mechanisms

4.1 Inducing Factors

Rock avalanche is generally triggered by some inducing factors such as rainstorm or mining under given geological environment. The inducing factors can be divided into internal factors, including rock/soil type, geological structure and topography, and external factors such as rainstorm, groundwater and human activities. The internal factors generally govern the avalanche formation. For example, mining or engineering construction may accelerate the formation process of rock avalanche (Xing et al., 2016; Liu et al., 2017; Pradhan et al., 2019).

The study area has complicated terrain and landform, with great height difference, steep slopes in the upper part and gentle platform in the lower part, which provides adverse geometry conditions for slope deformation and failure.

The lithology in the study area is very complex, with developed karst and outcropped bedrock. Basically, the upper part is hard and the lower part is soft, with hard-soft interbedded strata. The strong dissolution against limestone on the top resulted in complicated voids. The soft rock is squeezed by the above hard rock due to gravity and weathering, leading to tensile stress zone and outward unloading fractures. The soft rock suffers from stronger weathering than hard rock, which may cause the hard rock fall down due to the loss of support.

Three sets of structural planes were developed, namely, ① N10 – 15°E/SE∠80 – 90°, ② N81 – 84°W/NE∠80 – 90°, and ③ N50 – 60°E/SE∠80 – 90°, which cut the rock mass in the source zone into various blocks. These structural planes finally slid due to several factors such as gravity and abundant dissolution cracks on the top of source zone.

The rainfall can seep into the rock mass through dissolution cracks and joints, softening the soft siltstone in the lower part and increasing the hydrostatic pressure, which decreased the slope stability. In addition, underground coal mining accelerated the generation of rock avalanche.

4.2 Failure Mechanism

The field survey and detailed analysis results indicated that the steep and high terrain, complex lithology, developed karst and outcropped bedrock jointly provided the potential energy and material source. The abundant joints and cracks were the adverse geometric conditions, and the rainfall and mining accelerated the occurrence of rock avalanche. The inferred evolution of Pusa

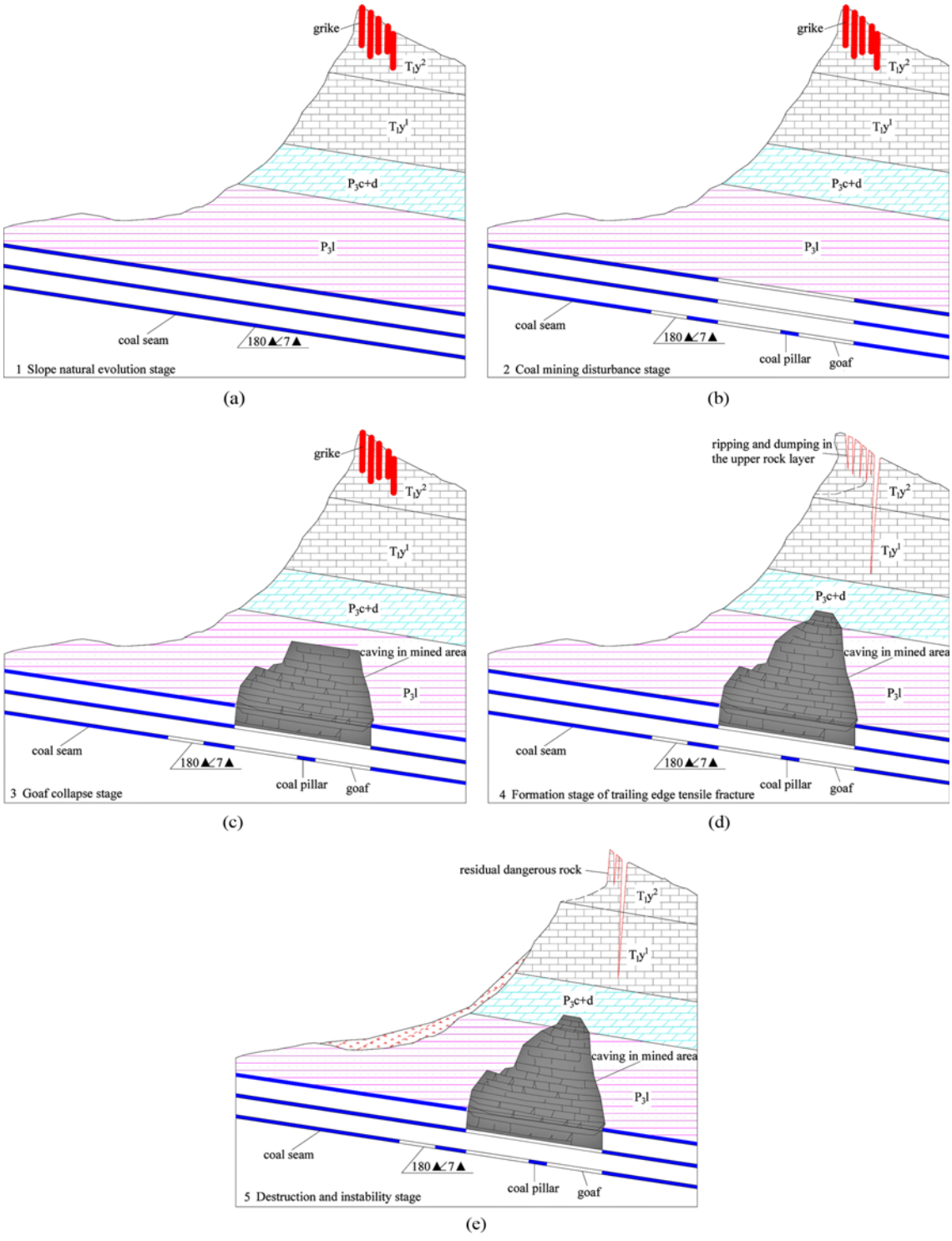

Fig. 7. Inferred Evolution Process of Pusa Avalanche: (a – e) The Process of Formation and Destruction of Rock Avalanche after Surface Deformation Caused by Underground Mining

avalanche is shown in Fig. 7.

5. Numerical Simulation on Dynamic Process

After collision, the collapse was transformed into rock avalanche in the form of debris flow, and moved downward quickly, with the length in flow direction greatly larger than thickness. Thus, the Pusa avalanche was analyzed by the long-wave scaling method which has been widely applied to solve the continuum flow model of gravitational avalanche (Savage and Hutter, 1989; Iverson and Denlinger, 2001; Mangeney-Castelnau, 2003; Christen et al., 2010; Mahboob et al., 2015; Bai and He, 2020). Savage and

Hutter (1989) has derived one dimensional depth-averaged equations, and applied these equations to actual topographies and higher dimensions (McDougall and Hungr, 2005; Pudasaini and Hutter, 2007; Luna et al., 2012). The local coordinate system (Christen et al., 2010) was applied in this paper, and the corresponding gravitational acceleration components at various points were calculated on the base of the terrain before rock avalanche debris flow happened.

5.1 Governing Equations

Field survey showed that the rock avalanche debris flow had a scraping effect, and the detached rocks collided strongly against the accumulation zone where the terrain is like a platform with low sides. The terrain separated the avalanche into two branches after collision. The governing equations for simulating the dynamic process of Pusa rock avalanche debris flow after collision include the erosion item and topography item because the flow was largely affected by the erosion and terrain during movement. Thus, the depth-averaged mass and momentum conservation equations during movement can be written as

$$\frac{\partial h}{\partial t}+\frac{\partial hu}{\partial x}+\frac{\partial hv}{\partial y}=E\,, \tag{1}$$

$$\frac{\partial hu}{\partial t}+\frac{\partial (hu^2+\frac{1}{2}k_{ap}g_z h^2)}{\partial x}+\frac{\partial huv}{\partial y}=g_x h-\frac{\tau_{bx}}{\rho}-k_{ap}g_z h\frac{\partial Z}{\partial x}+u_b E\,, \tag{2}$$

$$\frac{\partial hu}{\partial t}+\frac{\partial huv}{\partial x}+\frac{\partial (hv^2+\frac{1}{2}k_{ap}g_z h^2)}{\partial y}=g_y h-\frac{\tau_{by}}{\rho}-k_{ap}g_z h\frac{\partial Z}{\partial y}+v_b E\,, \tag{3}$$

where E denotes the erosion rate, h denotes the avalanche thickness, u denote the x-direction velocity, v denote the y-direction velocity, ρ denotes the avalanche density, and $Z(x, y)$ denotes the basal topography during avalanche movement.

The right-side terms of Eqs. (2) and (3) are the external forces. The k_{ap} is the lateral pressure coefficient, and is written as

$$k_{ap}=2\frac{1\pm\left[1-\cos^2\phi_{\text{int}}(1+\tan^2\phi_{bed})\right]^{\frac{1}{2}}}{\cos^2\phi_{\text{int}}}-1\,, \tag{4}$$

where ϕ_{int} is the angle of internal friction of avalanche, ϕ_{bed} is the bed friction angle of avalanche, "+" represents the passive state ($\partial u/\partial x+\partial v/\partial y\le 0$) and "–" represents the active state ($\partial u/\partial x+\partial v/\partial y\ge 0$). τ_{bi}, $i\in[x,y]$ is the x- and y-direction frictions from rock avalanche debris flow, respectively, which can be expressed by

$$\tau_{bi}=\frac{\upsilon_i}{\|\mathbf{u}\|}\left(\rho g_z h\mu+R_t\mathbf{u}^2\right),\quad R_t=\mu h\frac{\mathbf{u}^T K\mathbf{u}}{\mathbf{u}^2}\,, \tag{5}$$

where $\upsilon_i=[u,v]^T, i\in[x,y]$ splits the total friction into a velocity independent dry-Coulomb term proportional to the normal stress at the avalanche bottom (friction coefficient μ) and a velocity dependent turbulent and viscous friction; R_t is the resistance related to the terrain of contact surface and field variables such as velocity and height; K is the full curvature tensor of terrain (Christen et al., 2010; Moretti et al., 2015) affecting the fluid motion during movement, which can be written by

$$K=\begin{pmatrix}K_x & K_{xy}\\ K_{xy} & K_y\end{pmatrix}. \tag{6}$$

In Eq. (6), K_x, K_{xy} and K_y can be expressed as

$$K_x=\frac{\partial_x^2 Z}{\left(1+\partial_x Z^2\right)\sqrt{1+\partial_x Z^2+\partial_y Z^2}}\,,$$

$$K_{xy}=\frac{\partial_x\partial_y Z}{\sqrt{1+\partial_x Z^2}\sqrt{1+\partial_y Z^2}\sqrt{1+\partial_x Z^2+\partial_y Z^2}}\,,$$

$$K_y=\frac{\partial_y^2 Z}{\left(1+\partial_y Z^2\right)\sqrt{1+\partial_x Z^2+\partial_y Z^2}}\,.$$

5.2 Erosion Model

Surface erosion acts as an important part in landform evolution. Compared with the erosion by long-term weathering and overland flow, the erosion by collapse, rock avalanche and flow debris may transform the landform just in minutes or dozens of seconds. The collapse, rock avalanche and flow debris not only transform the landform but also affect their own movement. For example, the erosion can increase the avalanche volume, which enhances the damage to downstream region. To study such phenomenon, scholars provided various erosion models in recent years (McDougall and Hungr, 2005; Iverson, 2012; Luna et al., 2012; Ouyang et al., 2015). Since the formula about erosion rate should match boundary momentum jump condition, the erosion model in Iverson and Ouyang et al. (2015) was used in this paper, which can be described as

$$E=\frac{\tau_b-\tau_s}{\rho\sqrt{u^2+v^2}}\,, \tag{7}$$

where τ_b is the total basal traction from avalanche, τ_s is the total shear stress from erodible bed. Here $\tau_b=\rho g_z h\tan\varphi_b$ where φ_b is the angle of internal friction of rock avalanche, and $\tau_s=c+\rho(1-s)g_z h\tan\varphi_s$ where c is the cohesion of erodible bed, φ_s is the angle of internal friction of erodible bed, and s is the ratio of excess pore water pressure to hydrostatic pressure ranging from 0 to 1. Here s can represent the liquefaction extent of basal bed.

5.3 Results and Discussion

Equations (1) to (3) were solved with finite volume method of weighted essentially non-oscillatory scheme and Harten-Lax-van Leer-contact (HLLC) approximation Riemann solver (Liang and Borthwick, 2009; Coralic and Colonius, 2014). By numerical simulations, the thickness and velocity of Pusa rock avalanche-debris flow at various times were simulated, as shown in Figs. 8 – 9. Owing to Pusa avalanche is strictly a rock avalanche-debris flow, which is different from general soil landslide, we are more likely to study the influence of the bottom friction coefficient on the movement process than the internal friction angle. Therefore,

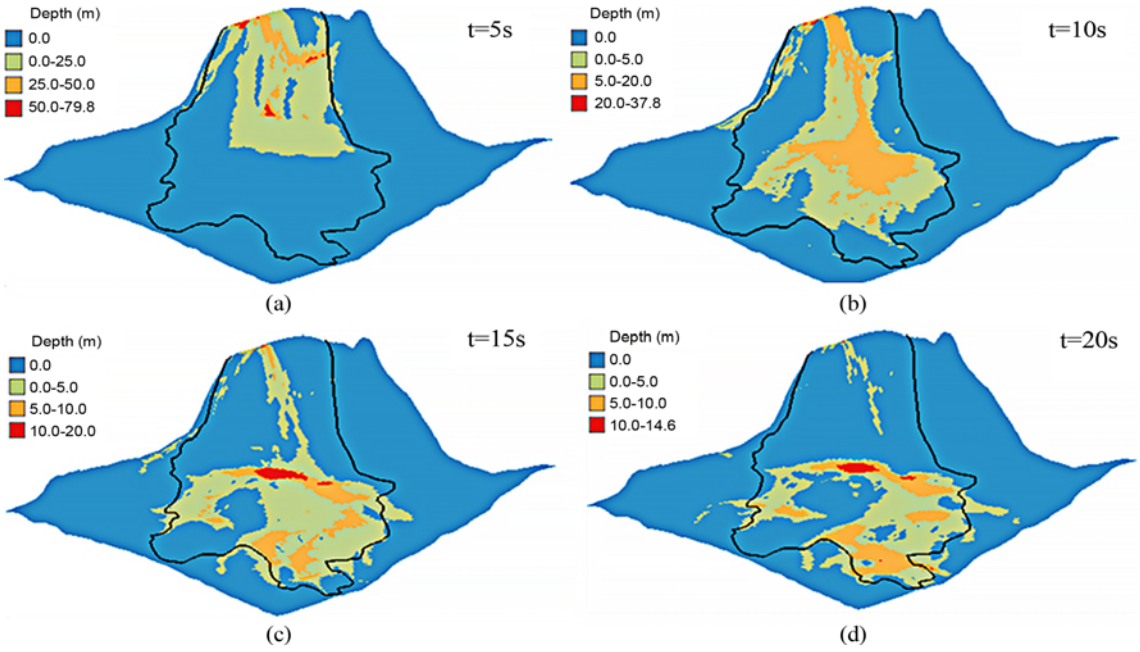

Fig. 8. Thickness of Pusa Avalanche at Various Times by Numerical Simulation: (a) The Accumulation Thickness Figure at 5s, (b) The Accumulation Thickness Figure at 10s, (c) The Accumulation Thickness Figure at 15s, (d) The Accumulation Thickness Figure at 20s

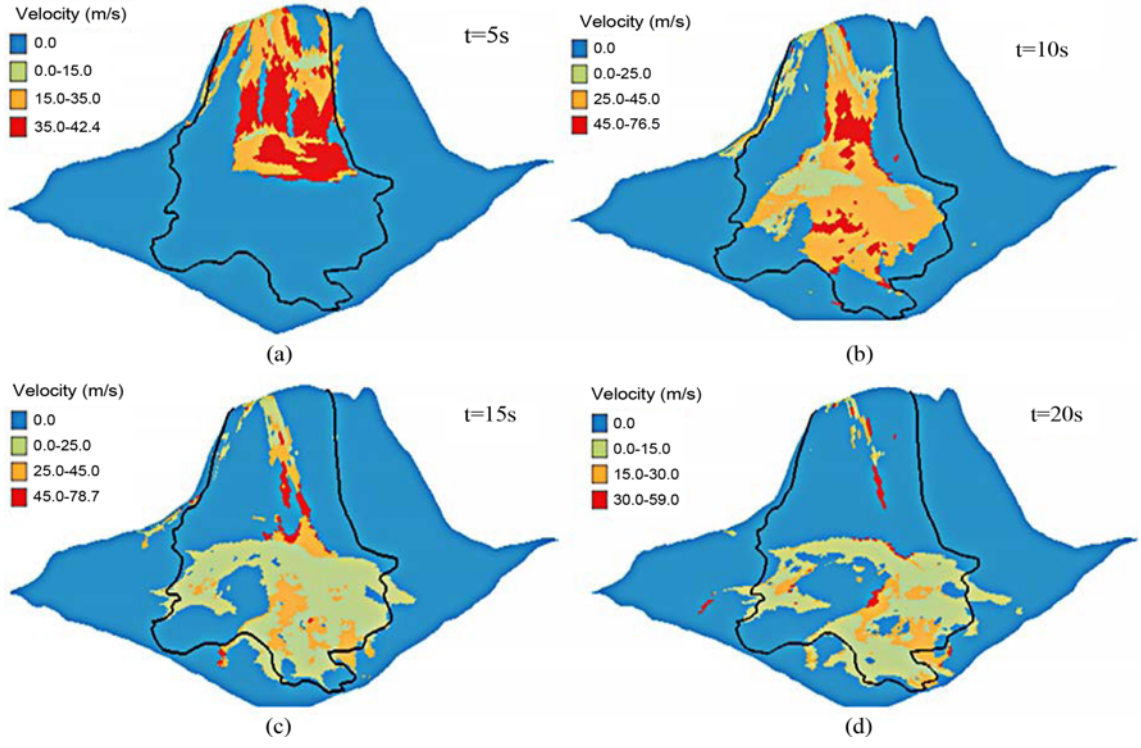

Fig. 9. Velocity of Pusa Avalanche at Various Times by Numerical Simulation: (a) The Movement Velocity Figure at 5s, (b) The Movement Velocity Figure at 10s, (c) The Movement Velocity Figure at 15s, (d) The Movement Velocity Figure at 20s

in the subsequent simulation process, the internal friction angle is selected as a constant value (35°). As we all know most of the potential energy of rock avalanche-debris flow is consumed by ground friction during movement. Meanwhile, due to the disintegration of Pusa rock avalanche in the process of dumping, impact with the ground and subsequent fragmentation in the process of movement, they all have energy consumption, especially the impact process with the ground during dumping, which could not be reflected in our physical model. Therefore, we choose different friction coefficients (fric = 0.84, 0.82, 0.80, 0.78) that may be larger than the actual situation to simulate the influence of its motion process (Figs. 10 – 11). The simulation results show

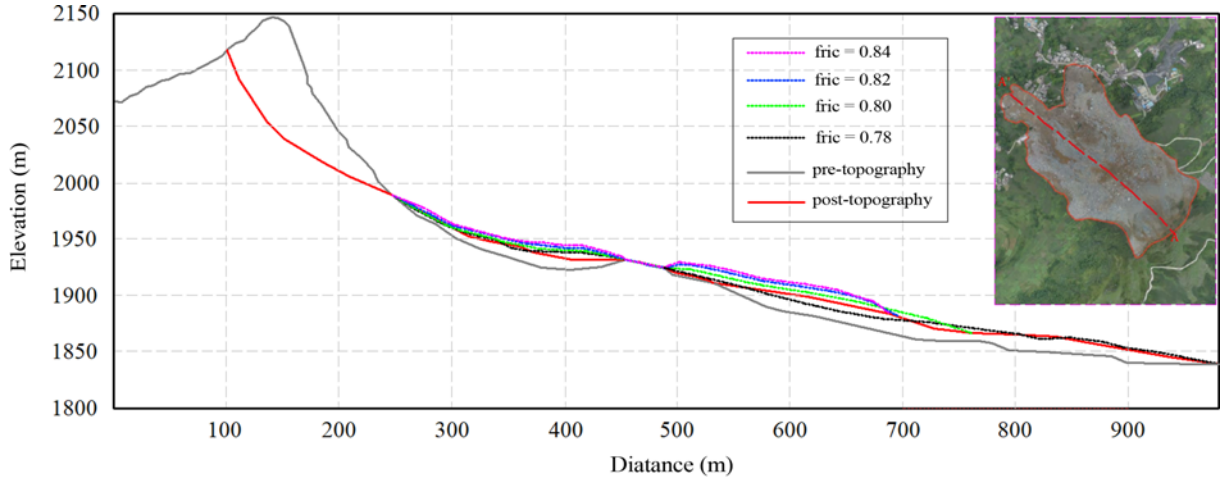

Fig. 10. Comparison Profile of Accumulation Depth of Pusa Avalanche under Four Different Bottom Friction Coefficient Simulations at Φ_{int} = 35°

that if a large friction coefficient is selected to consume potential energy, the debris flow may stop moving early. Therefore, we need to try new friction coefficient values so that the simulation results are close to the field investigation results, more importantly, we need to constantly improve the motion physical model to consider more physical mechanisms. Otherwise, it is difficult to select appropriate parameter values in the future simulation process.

By selecting different friction coefficient values, when the friction coefficient is 0.78, the numerically simulated results are generally consistent with the measured accumulation of rock-avalanche-debris flow in the field. However, there are still shortcomings, for instance, the simulated duration is shorter than that from video, and the velocity is larger than that from video because

1. The depth-averaged equations neglect the variation of velocity with depth.
2. The dynamic progress behaved a complicated progressive failure with rock disintegration and strong collision. For example, the velocity at t = 5s was up to 35 m/s in Fig. 9, which must consume some potential energy. However, the disintegration and collision of rock mass are not considered in the physical model. Therefore, the simulated velocity and thickness are larger than the measured results.
3. As shown in Fig. 9, even the region far away from the source zone had a velocity of about 15 m/s at t = 20s because of μ = 0.78 and the neglect of some energy consumption. In addition, μ varies greatly with location, and the rock disintegration and collision against residential houses necessarily consumed some energy.
4. The terrain data measured in 2016 were used to determine the volume of avalanche source, but historical remote sensing data indicated that some collapse had occurred during the period from April 2017 to July 2017. Furthermore, the Pusa avalanche featured a progressive failure, so the avalanche volume, determined by the difference between terrain data before and after this accident, was slightly greater than the actual volume. Although the model based on the depth-averaged equations is less than satisfactory to some extent, it could still be a better way to quantitatively analyze the dynamic process of rock avalanche debris flow.

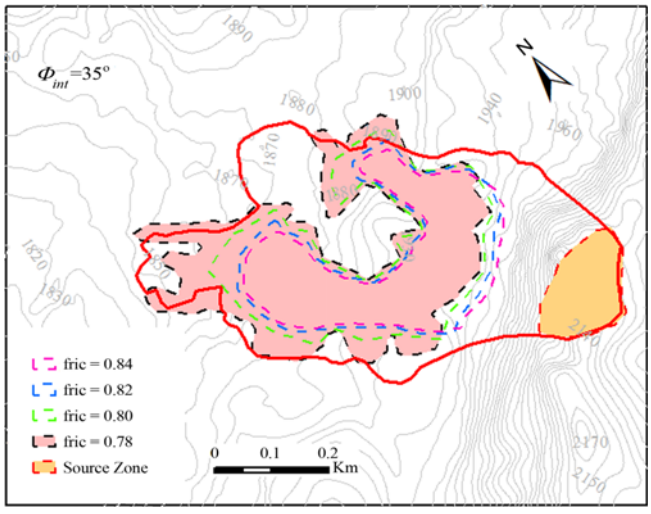

Fig. 11. Comparison of Pusa Rock Avalanche-Debris Flow Accumulation Characteristics under Four Different Bottom Friction Coefficient Simulations at Φ_{int} = 35°

6. Conclusions

Based on the geological & topographic conditions and field survey, the failure mechanism was analyzed and the dynamic process was simulated for Pusa avalanche. Thus, the following conclusions were obtained: 1) the tail cracks were triggered by adverse geological conditions, steep slope, coal mining, etc., with long period of critical stress state. The rainstorm finally accelerated the occurrence of rock avalanche; 2) the topography played an important role in avalanche evolution because the steep slope was natural free face, the deposit at slope toe buffered the collision, and the small platform divided the avalanche into

two branches; 3) the tail cracks became larger and the small-scale collapse happened before Pusa avalanche. Therefore, more attention should be paid to detailed investigation on potential dangerous blocks and deformed slope, and hence the disasters may be mitigated by engineering measures or buffer zones in an active way instead of passive disaster relief.

Acknowledgments

The authors would like to acknowledge the National Key Research and Development Program (Grant No. 2019YFC1509704), National Natural Science Foundation of China (Grant No. U1704243), High-level Talent Project of North China University of Water Resource and Electric Power (Grant No.201518), and Levee Safety and Disaster Prevention Engineering Research Center of Ministry of Water Resources.

ORCID

Not Applicable

References

Bai X, He S (2020) Dynamic process of the massive Aru glacier collapse in Tibet. *Landslides* 17(6):1353-1361, DOI: 10.1007/s10346-019-01337-x

Bozzano F, Lenti L, Martino S, Montagna A, Paciello A (2011) Earthquake triggering of landslides in highly jointed rock masses: Reconstruction of the 1783 Scilla rock avalanche (Italy). *Geomorphology* 129(3-4): 294-308, DOI: 10.1016/j.geomorph.2011.02.025

Chen L, Zhao C, Kang Y, Chen H, Yang C, Li B, Lu Y, Xing A (2020) Pre-event deformation and failure mechanism analysis of the Pusa landslide, China with Multi-Sensor SAR Imagery. *Remote Sensing* 12(5):856, DOI: 10.3390/rs12050856

Christen M, Kowalski J, Bartelt P (2010) RAMMS: Numerical simulation of dense snow avalanches in three-dimensional terrain. *Cold Regions Science and Technology* 63(1-2):1-14, DOI: 10.1016/j.coldregions.2010.04.005

Coralic V, Colonius T (2014) Finite-volume WENO scheme for viscous compressible multicomponent flows. *Journal of Computational Physics* 274:95-121, DOI: 10.1016/j.jcp.2014.06.003

Cox SC, McSaveney MJ, Spencer J, Allen SK, Ashraf S, Hancox GT, Sirguey P, Salichon J, Ferris BG (2015) Rock avalanche on 14 July 2014 from Hillary Ridge, Aoraki/Mount Cook, New Zealand. *Landslides* 12(2):395-402, DOI: 10.1007/s10346-015-0556-7

Dai FC, Tu XB, Xu C, Gong QM, Yao X (2011) Rock avalanches triggered by oblique-thrusting during the 12 May 2008 Ms 8.0 Wenchuan earthquake, China. *Geomorphology* 132(3-4):300-318, DOI: 10.1016/j.geomorph.2011.05.016

Fan X, Xu Q, Scaringi G, Zheng G, Huang R, Dai L, Ju Y (2019) The "long" runout rock avalanche in Pusa, China, on August 28, 2017: A preliminary report. *Landslides* 16(1):139-154, DOI: 10.1007/s10346-018-1084-z

Haque U, da Silva PF, Devoli G, Pilz J, Zhao B, Khaloua A, Wilopo W, Andersen P, Lu P, Lee J, Yamamoto T, Keellings D, Wu JH, Glass GE (2019) The human cost of global warming: Deadly landslides and their triggers (1995-2014). *Science of the Total Environment* 682:673-684, DOI: 10.1016/j.scitotenv.2019.03.415

He S, Bai X, Ouyang C, Wang D (2017) On the survey of giant landslide at Xinmo Village of Diexi Town, Maoxian Country, Sichuan Province, China. *Mountain Research* 35(4):598-603 (in Chinese)

Hewitt K (2009) Rock avalanches that travel onto glaciers and related developments, Karakoram Himalaya, Inner Asia. *Geomorphology* 103(1):66-79, DOI: 10.1016/j.geomorph.2007.10.017

Huang R (2004) Mechanism of large scale landslides in western China. *Advances in Earth Science* 19(3):443-451 (in Chinese)

Iverson RM (2012) Elementary theory of bed-sediment entrainment by debris flows and avalanches. *Journal of Geophysical Research: Earth Surface* 117(F3), DOI: 10.1029/2011jf002189

Iverson RM, Denlinger RP (2001) Flow of variably fluidized granular masses across three-dimensional terrain: 1. Coulomb mixture theory. *Journal of Geophysical Research: Solid Earth* 106(B1):537-552, DOI: 10.1029/2000jb900329

Jibson RW, Harp EL, Schulz W, Keefer DK (2006) Large rock avalanches triggered by the M 7.9 Denali Fault, Alaska, earthquake of 3 November 2002. *Engineering Geology* 83(1-3):144-160, DOI: 10.1016/j.enggeo.2005.06.029

Li X, Zhang N, Sheng Z, Li S, Hao J (2020) Sliding mechanisms and fracture genesis of Jiweishan landslide in Wulong. *Chinese Journal of Rock Mechanics and Engineering* 39(1):1-12 (in Chinese)

Liang Q, Borthwick AG (2009) Adaptive quadtree simulation of shallow flows with wet-dry fronts over complex topography. *Computers & Fluids* 38(2):221-234, DOI: 10.1016/j.compfluid.2008.02.008

Liu Y, Liu X, Lu Y, Li X, Li P (2017) Numerical analysis of evaluation methods and influencing factors for dynamic stability of bedding rock slope. *Journal of Vibroengineering* 19(3):1937-1961, DOI: 10.21595/jve.2016.17210

Luna BQ, Remaître A, van Asch TWJ, Malet JP, van Westen CJ (2012) Analysis of debris flow behavior with a one dimensional run-out model incorporating entrainment. *Engineering Geology* 128:63-75, DOI: 10.1016/j.enggeo.2011.04.007

Mahboob MA, Iqbal J, Atif I (2015) Modeling and simulation of glacier avalanche: A case study of Gayari sector glaciers hazards assessment. *IEEE Transactions on Geoscience and Remote Sensing* 53(11), DOI: 10.1109/TGRS.2015.2419171

Mangeney-Castelnau A (2003) Numerical modeling of avalanches based on Saint Venant equations using a kinetic scheme. *Journal of Geophysical Research* 108(B11), DOI: 10.1029/2002jb002024

McDougall S, Hungr O (2005) Dynamic modelling of entrainment in rapid landslides. *Canadian Geotechnical Journal* 42(5):1437-1448, DOI: 10.1139/t05-064

Moretti L, Allstadt K, Mangeney A, Capdeville Y, Stutzmann E, Bouchut F (2015) Numerical modeling of the Mount Meager landslide constrained by its force history derived from seismic data. *Journal of Geophysical Research: Solid Earth* 120(4):2579-2599, DOI: 10.1002/2014jb011426

Ouyang C, He S, Tang C (2015) Numerical analysis of dynamics of debris flow over erodible beds in Wenchuan earthquake-induced area. *Engineering Geology* 194:62-72, DOI: 10.1016/j.enggeo.2014.07.012

Pirulli M (2009) The Thurwieser rock avalanche (Italian Alps): Description and dynamic analysis. *Engineering Geology* 109(1-2):80-92, DOI: 10.1016/j.enggeo.2008.10.007

Pradhan SP, Panda SD, Roul AR, Thakur M (2019) Insights into the recent Kotropi landslide of August 2017, India: A geological investigation and slope stability analysis. *Landslides* 16(8):1529-1537, DOI: 10.1007/s10346-019-01186-8

Pudasaini SP, Hutter K (2007) Avalanche dynamics dynamics of rapid flows of dense granular avalanches. Springer Science & Business Media, Berlin, Germany

Savage BSB, Hutter K (1989) The motion of a finite mass of granular material down a rough incline. *Journal of Fluid Mechanics* 199:177-215, DOI: 10.1017/S0022112089000340

Smith GM, Davies TR, McSaveney MJ, Bell DH (2005) The Acheron rock avalanche, Canterbury, New Zealand — morphology and dynamics. *Landslides* 3(1):62-72, DOI: 10.1007/s10346-005-0012-1

Socco LV, Jongmans D, Boiero D, Stocco S, Maraschini M, Tokeshi K, Hantz D (2010) Geophysical investigation of the Sandalp rock avalanche deposits. *Journal of Applied Geophysics* 70(4):277-291, DOI: 10.1016/j.jappgeo.2009.12.005

Wu J-H, Chen J-H, Lu C-W (2013) Investigation of the Hsien-du-Shan rock avalanche caused by typhoon Morakot in 2009 at Kaohsiung county, Taiwan. *International Journal of Rock Mechanics and Mining Sciences* 60:148-159, DOI: 10.1016/j.ijrmms.2012.12.033

Xiao R, Chen H, Leng Y, Wei Y, Wang W (2018) Preliminary analysis on the failure process and mechanism of the August 28 collapse in Nayong County, Guizhou Province. *The Chinese Journal of Geological Hazard and Control* 29(1):2-9, DOI: 10.16031/j.cnki.issn.1003-8035.2018.01.02 (in Chinese)

Xing A, Yuan X, Xu Q, Zhao Q, Huang H, Cheng Q (2016) Characteristics and numerical runout modelling of a catastrophic rock avalanche triggered by the Wenchuan earthquake in the Wenjia valley, Mianzhu, Sichuan, China. *Landslides* 14(1):83-98, DOI: 10.1007/s10346-016-0707-5

Xu Q, Li W, Dong X, Xiao X, Fan X, Pei X (2017) The Xinmocun landslide on June 24, 2017 in Maoxian, Sichuan characteristics and failure mechanism. *Chinese Journal of Rock Mechanics and Engineering* 36(11):2612-2628 (in Chinese)

Yin Y (2010) Mechanism of apparent dip slide of inclined bedding rockslide: A case study of Jiweishan rockslide in Wulong, Chongqing. *Chinese Journal of Rock Mechanics and Engineering* 29(2):217-227 (in Chinese)

Zambrano OM (2007) Large rock avalanches: A kinematic model. *Geotechnical and Geological Engineering* 26(3):283-287, DOI: 10.1007/s10706-007-9164-1

Zhu HP, Wu YH, Yu AB (2005) Discrete and continuum modelling of granular flow. *China Particuology* 3(6):354-363, DOI: 10.1016/s1672-2515(07)60215-2